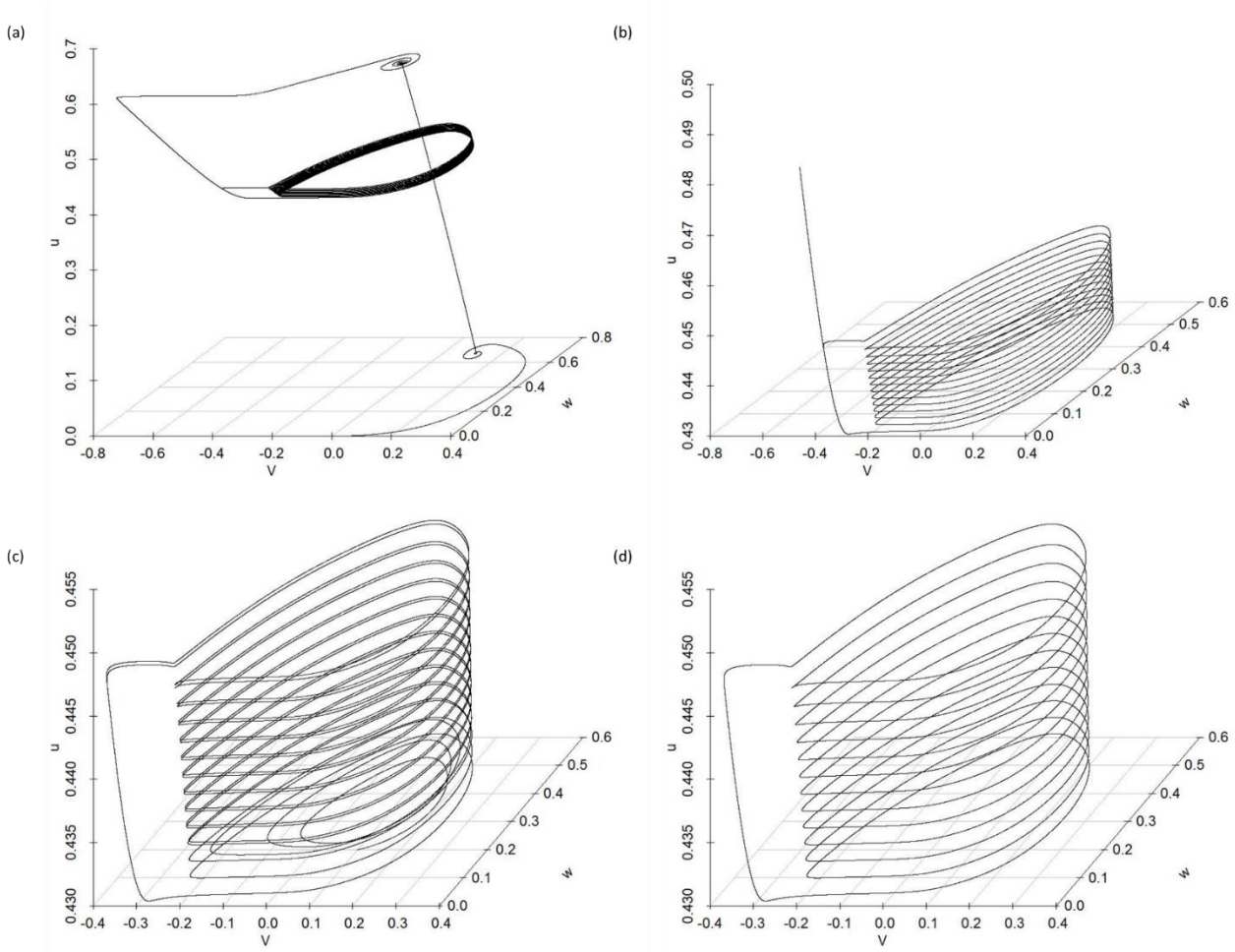

Figure 1. The 3-D plots showing the changes in V, w, and u across time. Time is implicit in the diagrams. (a) The phase portrait for the initial state of V=0, w=0, and u=0, for (0-3000) time range. (b) The zoomed-in plot in (a) focuses on the (2100-3000) time range. (c) The phase portrait for the initial state of V=0.1, w=0.2, and u=0.43 is for (0-3000). (d) The zoomed-in version of the plot in (c) focusing on the (2100-3000) time range.

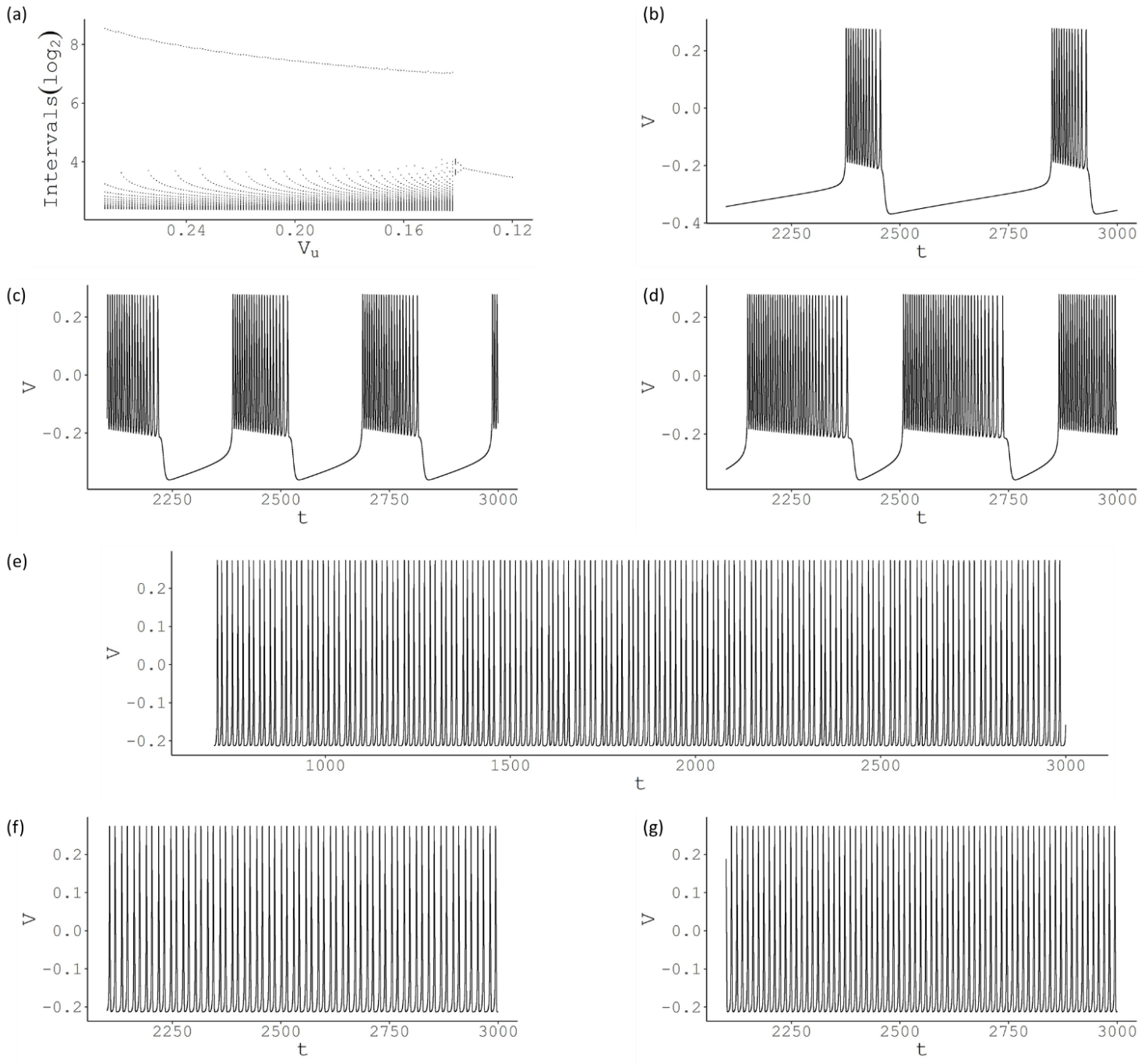

Figure 2. The change in firing behaviour for various values of V_u. (a) For high values of V_u, a large interval between spikes is observed that shows the period between bursts and many short intervals for the spikes within the bursts. Around 0.14 value, it reaches a chaotic region before switching to period-2 and period-1 bursting. The plot is displayed in log scale, and the x-axis is in descending order to be consistent with the original article. (b) Membrane potential (V) is plotted against time t for $V_u = 0.272$. Large inter-burst intervals and 13 spikes per burst are observed. (c) The number of spikes per bursts increases to 21, and inter-burst intervals decrease for $V_u = 0.2$. (d) When Vu reaches 0.145, there are 36 spikes per burst. (e) For $V_u = 0.1415$, no bursting behaviour is observed with chaotic intervals. (f) The period-2 pattern is reached with $V_u = 0.14$. (g) The period-1 pattern is reached with $V_u = 0.13$.

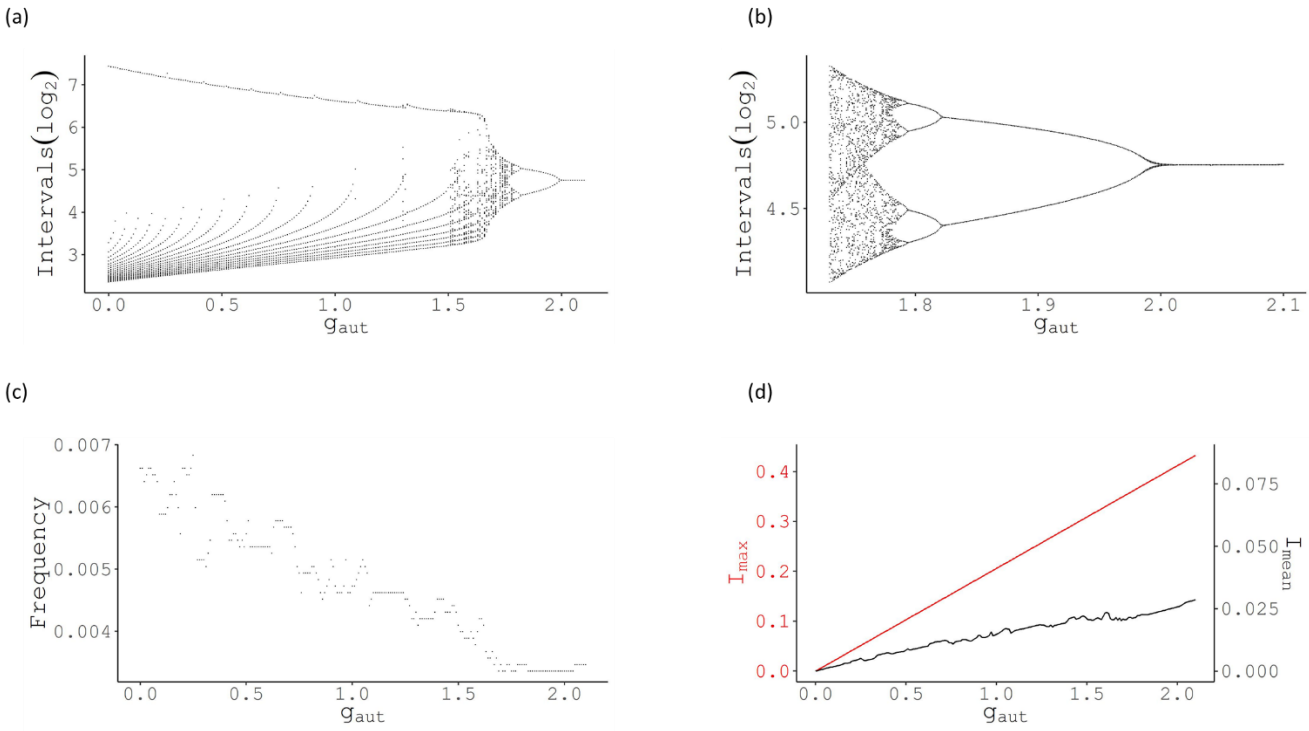

Figure 3. The change in firing behaviour for various values of g_{aut}. (a) For low values of g_{aut}, a large interval between spikes is observed that shows the period between bursts and the number of short intervals for the spikes within the bursts. Around 1.7 value, it reaches a chaotic region before switching to period-8, period-4, period-2 and period-1 bursting. The plot is displayed in the log scale. (b) The zoomed-in version of the plot in (a) shows the chaotic to periodic transition. (c) The frequency of spikes shows a decreasing trend with increasing g_{aut}. (d) Both I_{mean} and I_{max} increase as g_{aut} increases.

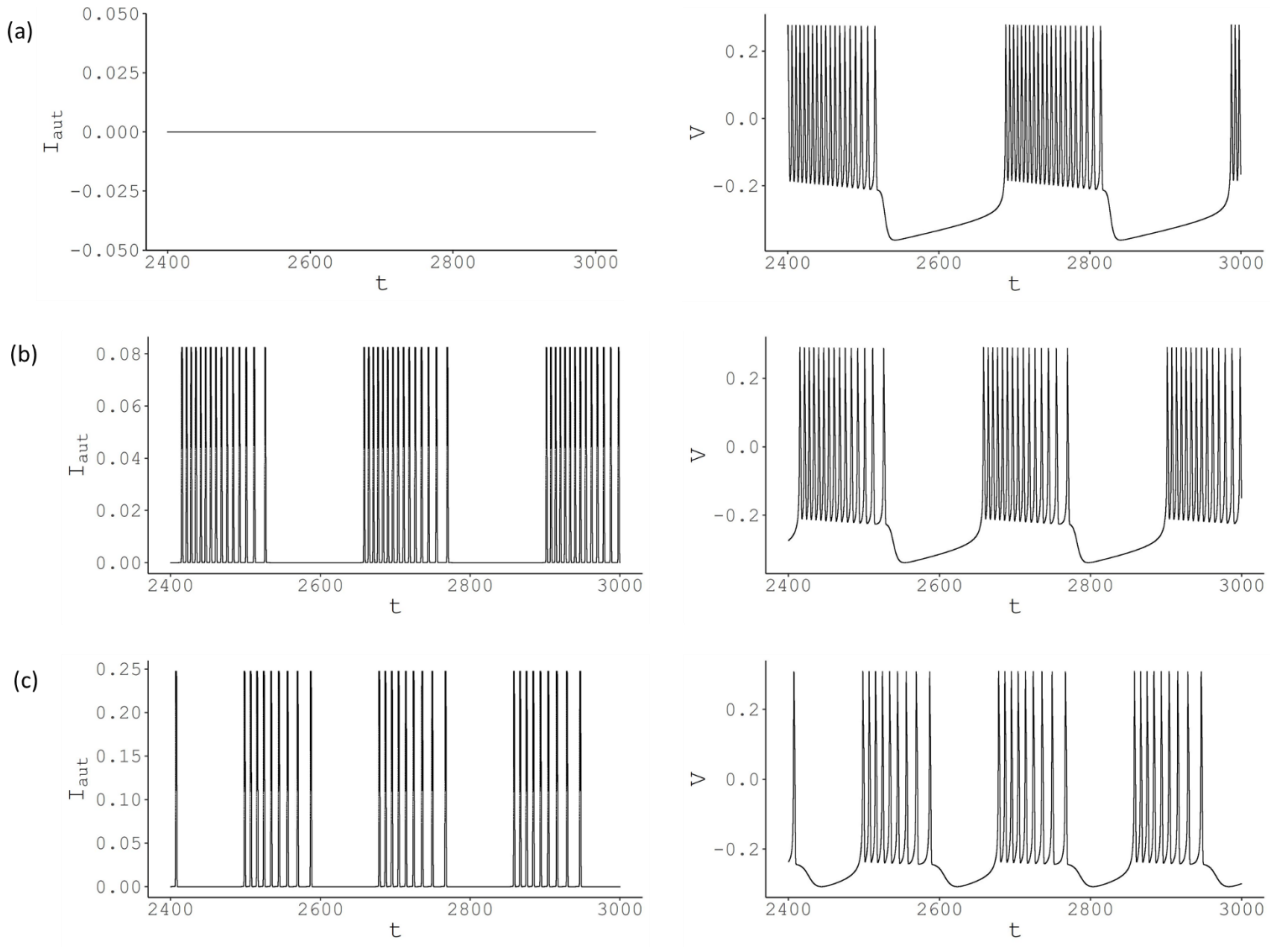

Figure 4. The bursting behaviour observed for various values of g_{aut}. (a) g_{aut} = 0, ((b) g_{aut} = 0.4, (c) g_{aut} = 1.2. The left-hand side graphs show the current, right-hand side graphs display the membrane potentials. The value of I_{aut} increases with g_{aut}, as seen by the scale change of the y-axes.

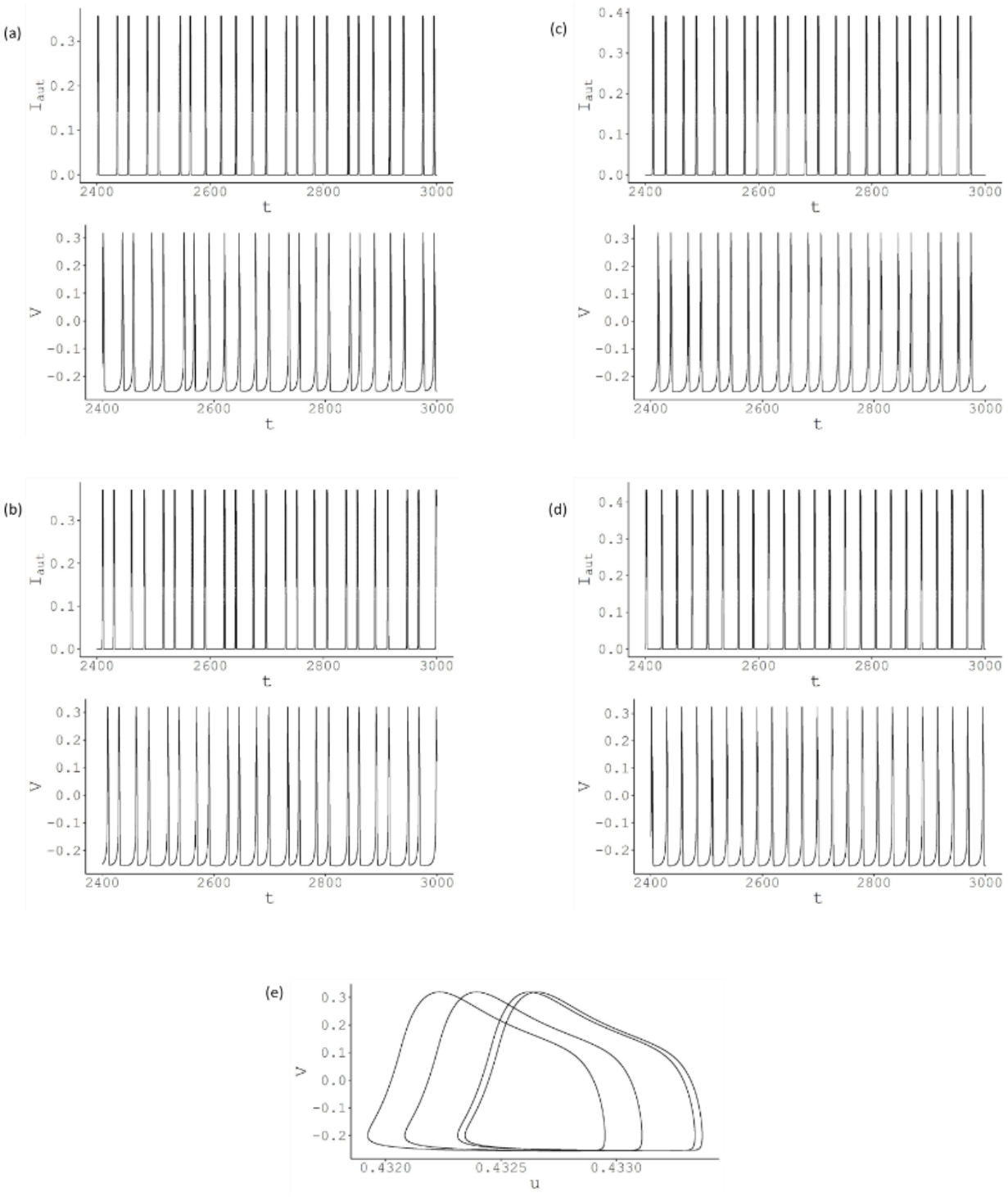

Figure 5. The spiking behaviour observed for various values of g_{aut}. (a) g_{aut} = 1.73, (b) g_{aut} = 1.8, (c) g_{aut} = 1.9 (d) g_{aut} = 2.1. The top graphs show the current, and the bottom graphs display the membrane potentials. The value of I_{aut} increases with g_{aut}, as seen by the scale change of the y-axes. (e) The phase portrait of V versus u for g_{aut} = 1.8.